Journal of Power and Energy Engineering, 2024, 12, 44-60
https://www.scirp.org/journal/jpee
ISSN Online: 2327-5901
ISSN Print: 2327-588X

Coordination of Regulation Devices for Damping Power Oscillations in a Dynamic Disturbance Context: A Fuzzy Logic-Based Approach Applied to the Electrical Grid of the Republic of Congo

Mavie Grace Mimiesse[1*], Davy Rostand Souamy Loembe[1], Smaël Magloire Elombo Motoula[2], Désiré Lilongo-Boyenga[1]

[1]Laboratoire du Génie Électrique et Électronique, École Nationale Supérieure Polytechnique, Université Marien NGOUABI, Brazzaville, Congo
[2]Institut Supérieur d'Architecture, Urbanisme, Bâtiment et Travaux Punlics, Université Dénis, SASSOU-N'GUESSO, Kintelé, Congo
Email: *lucianamimiesse@gmail.com

How to cite this paper: Mimiesse, M.G., Loembe, D.R.S., Motoula, S.M.E. and Lilongo-Boyenga, D. (2024) Coordination of Regulation Devices for Damping Power Oscillations in a Dynamic Disturbance Context: A Fuzzy Logic-Based Approach Applied to the Electrical Grid of the Republic of Congo. *Journal of Power and Energy Engineering*, **12**, 44-60.
https://doi.org/10.4236/jpee.2024.121004

Received: December 13, 2023
Accepted: January 28, 2024
Published: January 31, 2024

Abstract

This article presents a fuzzy logic-based approach to coordinate the control devices of the power system, such as Power System Stabilizers (PSS) and Static Synchronous Compensators (STATCOM), to damp power oscillations caused by dynamic disturbances. At first, we used the Lyapunov method to study the dynamic stability of the power grid in the Republic of Congo. This method allowed us to analyze the eigenvalues of the state variable matrix and highlight the eigenvalues in the complex plane. Secondly, we proposed a fuzzy logic-based controller to account for uncertainties existing near the thresholds. The inputs to this controller are the generator speed and generator rotor angle. We demonstrated the effectiveness and feasibility of this fuzzy control by applying it to the power grid of the Republic of Congo, with three power stabilizers and two STATCOMs.

Keywords

Fuzzy Logic, STATCOM, PSS, Lyapunov, Republic of Congo

1. Introduction

In the current context marked by a high demand on electrical grids, approaching

their operational safety limits, electric power distribution companies are facing significant challenges. These challenges encompass the effective management of energy flows, the maintenance of appropriate voltage levels, and other complex operational issues. In this context, safety takes on crucial importance. The emergence of Flexible AC Transmission System (FACTS) devices represents a significant advancement, offering increased opportunities for intensive network utilization voltage, and impedance [1] [2]. These devices enable more precise power flow management and improved voltage regulation, thereby increasing network stability margins or approaching the thermal limits of transmission lines. Furthermore, due to their responsiveness to electrical grid fluctuations, FACTS devices have proven to be effective in dampening electromechanical oscillations, working in conjunction with Power System Stabilizers (PSS). These PSS devices, by detecting variations in rotor speed or electrical power of generators, transmit an appropriate signal to the Automatic Voltage Regulator (AVR), allowing the generator to produce additional damping torque, thus counteracting the adverse effects of the excitation system on network oscillations [3] [4]. However, when multiple control devices, including FACTS and Power System Stabilizers (PSS), are integrated into electrical grids, interactions can occur between FACTS devices, between FACTS and PSS, as well as between FACTS and the loads connected to the network. These interactions result in low-frequency oscillations that significantly disrupt the stable operation of connected equipment, which should ideally operate steadily. To mitigate these low-frequency oscillations resulting from these interactions, various approaches have been proposed, including minimax methods, decentralized linear quadratic methods developed by J.C. Passelergue [5], and LMI-based methods developed by S. Ammari [6]. Fuzzy logic methods have also been employed to control FACTS devices, including SVC and STATCOM, with studies focusing on linearized models and nonlinear control approaches, especially for STATCOM [7]. Fuzzy logic methods have also been applied to control FACTS devices, including SVC and STATCOM [8]. The subject of this research is multidimensional. Therefore, the overall objective of this work is to stabilize the electrical grid of the Republic of Congo by mitigating low-frequency oscillations resulting from interactions between STATCOM devices for voltage support and PSS for power oscillation damping, using Lyapunov and fuzzy logic-based methods [9]. This study presents a major innovation as it is the first to be applied to the specific case of the electrical grid of the Republic of Congo, taking into account the presence of two STATCOMs and three PSS devices in the network. The structure of this article is as follows: Section 2 describes the power system stabilizer (PSS); Section 3 discusses the FACTS compensator model (STATCOM); Section 4 deals with the linearization of power systems; Section 5 is devoted to the modeling of fuzzy control; Section 6 presents the modeling of the Republic of Congo's electrical network; Section 7 shows the simulation results with and without control devices in the network. The effectiveness of fuzzy control in response to a disturbance in the Republic of Congo's network is demonstrated. Section 8 concludes this article.

2. Power System Stabilizer (PSS)

The block dedicated to the stabilization of the global power supply system offers the capability to regulate the oscillation of a synchronous machine's rotor by controlling its excitation. In an electrical context, disturbances within a given system can cause electromechanical oscillations in electric generators, commonly referred to as "power swings". It is imperative to effectively dampen these oscillations to ensure system stability, as highlighted in references [10] [11]. The signal generated by the Power System Stabilizer (PSS) is used as an additional input (denoted as vstab) to influence the excitation system block. The PSS input can take the form of the machine's rotational speed difference *dw* or the acceleration power *Pa* = *Pm* − *Pe*0 where *Pm* represents mechanical power and *Pe*0 represents electrical power [1] [12] [13]. **Figure 1** illustrates the schematic diagram of the power system stabilizer (PSS), which can be modeled using the following transfer function:

3. STATCOM Devices

The advanced Static Synchronous Compensator (STATCOM) represents a reactive power compensation device that integrates parallelly within the electrical system. Its main function is to produce or absorb reactive power, with the ability to regulate specific parameters of an electrical power network. It acts as a fully controllable reactive power source, allowing for the generation or absorption of reactive power as needed, using an electronic device for voltage processing and current waveform shaping within a Voltage Source Converter (VSC). **Figure 2** illustrates the schematic diagram of the STATCOM compensator, as presented in reference [14].

The current injected by the STATCOM is given by Equation (1) [14]:

$$\bar{I}_{sh} = \frac{\bar{V}_{sh} \cdot \bar{V}_k}{jX_K} \tag{1}$$

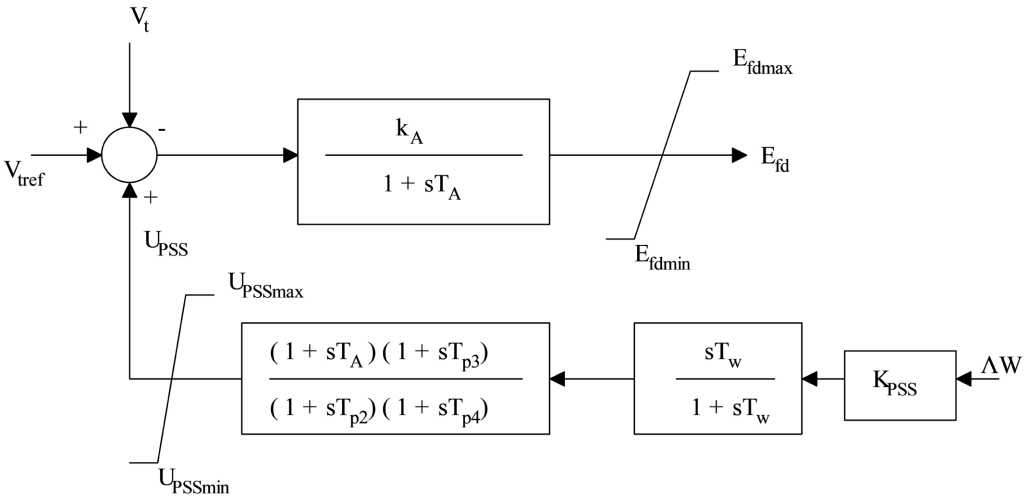

Figure 1. Diagram of the generic power system stabilizer.

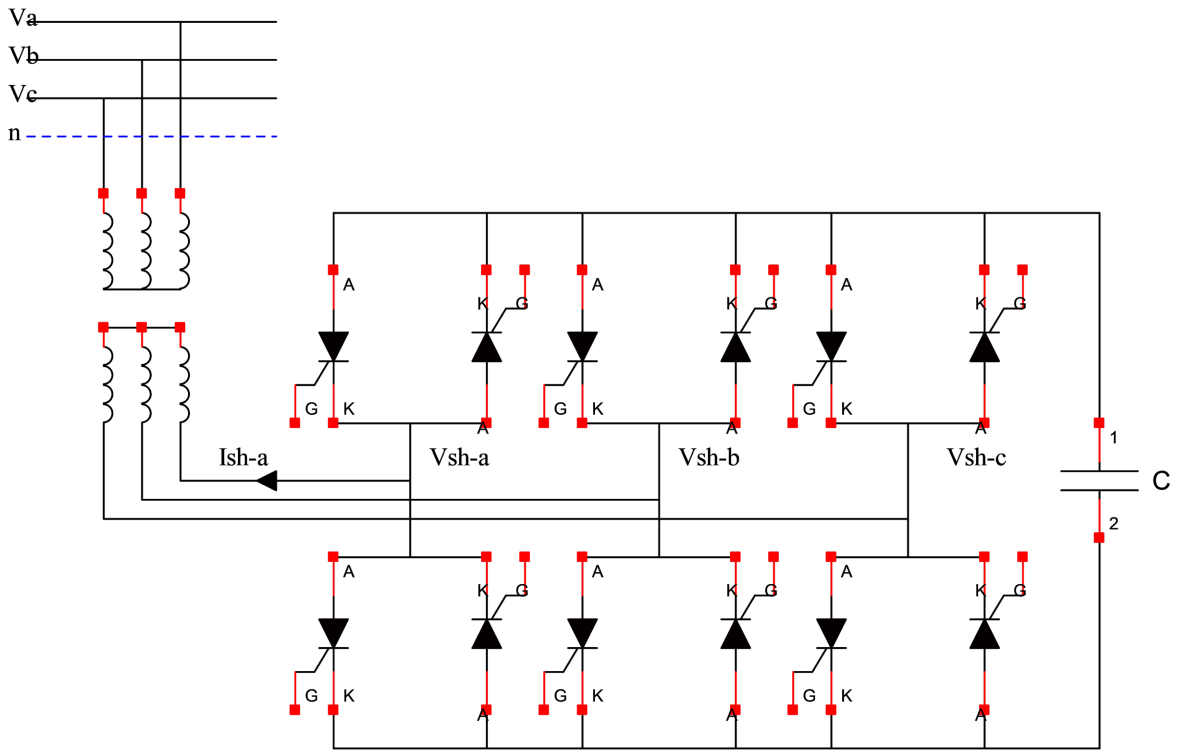

Figure 2. Block diagram of a statcom.

The injected power at the busbar is given by the following Equation (2):

$$\overline{S} = \overline{I}_{sh}^{*} \cdot \overline{V}_{k} = \frac{\overline{V}_{k}\left(\overline{V}_{k}^{*} \cdot \overline{V}_{sh}^{*}\right)}{-jX_{K}} = \frac{\overline{V}_{k}\left(\overline{V}_{k}^{*} \cdot \overline{V}_{sh}^{*} \cdot V_{k}^{2}\right)}{-jX_{K}} \tag{2}$$

We obtain the active and reactive power injected by the STATCOM at the busbar level using Equation (3) [15] [16].

$$\overline{S} = P_{sh} + jQ_{sh} \tag{3}$$

Si $\theta_{sh} = \theta$ (angle at the busbar connection), then active power is negligible, as shown by Equation (4) [15] [16].

$$\overline{S} \approx jQ_{sh} = j\frac{V_{k}\left[V_{sh} \cdot \cos\left(\theta_{k} - \theta_{sh}\right)\right]}{X_{K}} \tag{4}$$

4. Power System Linearization

In this section, we use the first Lyapunov-based small-signal theory method to establish the linear model of the multi-machine power system. The differential-algebraic equations governing the operation of a multi-machine electrical system are presented below according to the equations from (5)-(9) [16] [17]:

$$\frac{\mathrm{d}\delta_{i}}{\mathrm{d}t} = \omega_{i} - \omega_{s} \tag{5}$$

$$\frac{\mathrm{d}\dot{\omega}_{i}}{\mathrm{d}t} = \frac{T_{Mi}}{M_{i}} - \frac{E'_{qi} - X'_{di}I_{di}}{M_{i}} - \frac{E'_{di} - X'_{qi}I_{qi}}{M_{i}} - \frac{D\left(\omega_{i} - \omega_{s}\right)}{M_{i}} \tag{6}$$

$$\frac{\mathrm{d}E'_{qi}}{\mathrm{d}t} = -\frac{E'_{qi}}{T'_{di}} - \frac{\left(X_{di} - X'_{di}\right) I_{di}}{T'_{di}} + \frac{E_{fdi}}{T'_{di}} \tag{7}$$

$$\frac{\mathrm{d}E'_{di}}{\mathrm{d}t} = -\frac{E'_{di}}{T'_{di}} + \frac{I_{qi}\left(X_{qi} - X'_{qi}\right)}{T'_{di}} \tag{8}$$

$$\frac{\mathrm{d}E_{fdi}}{\mathrm{d}t} = \frac{1}{T_A}\left[-E_{fdi} + K_A V_{ref} - K_A\right] \tag{9}$$

Neglecting the electromotive force of the induced generator along the d axis, we obtain the linearized system of equations, represented by the equations from (10)-(13) [16]:

$$\Delta\dot{\delta}_i = \Delta\omega_i \tag{10}$$

$$\begin{aligned}\Delta\dot{\omega}_i = {} & \frac{1}{M_i}\Delta T_{Mi} - \frac{E'_{qi}}{M_i}\Delta I_{qi} + \frac{X'_{di} I_{di}}{M_i}\Delta I_{qi} + \frac{X'_{di} I_{di}}{M_i}\Delta I_{di} \\ & - \frac{I_{qi}}{M_i}\Delta E'_{qi} - \frac{X'_{qi} I_{di}}{M_i}\Delta I_{qi} - \frac{X'_{qi} I_{qi}}{M_i}\Delta I_{di}\end{aligned} \tag{11}$$

$$\Delta\dot{E}'_{qi} = -\frac{\Delta E'_{qi}}{T'_{di}} - \frac{\left(X_{di} - X'_{di}\right)\Delta I_{di}}{T'_{di}} + \frac{\Delta E_{fdi}}{T'_{di}} \tag{12}$$

$$\Delta\dot{E}_{fdi} = \frac{1}{T_{Ai}}\left[-\Delta E_{fdi} + K_{Ai} V_{ref} - K_{Ai}\right] \tag{13}$$

Given the presence of PSS (Power System Stabilizer) and STATCOM (Static Synchronous Compensator) controllers in a multi-machine electrical network, we will add four additional state variable equations, represented by equations (14)-(17) below [16]:

$$\Delta\dot{V}_{si} = -\frac{1}{T_2}\Delta V_{si} + \frac{K_{PSS}}{T_2}\frac{\Delta\omega_i}{\omega_s} + \frac{K_{PSS} T_1}{T_2}\frac{\Delta\dot{\omega}_i}{\omega_s} \tag{14}$$

$$\Delta\dot{X}_{s1} = -\frac{1}{T_m}\Delta X_{s1} + \frac{K_\omega}{T_m}\Delta\omega - \frac{1}{T_m}\Delta V_{meas} \tag{15}$$

$$\Delta\dot{X}_{s2} = \left(-\frac{K_P}{T_m} + K_1\right)\Delta X_{s1} + \frac{K_P K_\omega}{T_m}\Delta\omega - \frac{K_P}{T_m}\Delta V_{meas} \tag{16}$$

$$\Delta\dot{V}_{sc} = -\frac{1}{T_2}\Delta V_{sc} + \frac{1}{T_2}\Delta V_{s2} + \frac{T_1}{T_2}\Delta\dot{X}_{s2} \tag{17}$$

The linearized model of the multi-machine power system with PSS and STATCOM, described by Equations (10) of (17), is shown in **Figure 3**.

5. Fuzzy Control

Fuzzy logic offers the possibility of incorporating intelligence into the regulation of the speed and power of each generator. In this context, this mode of reasoning is particularly suitable for adjusting speed controls based on measured power and rotation levels. The regulator is capable of adjusting these setpoint values depending on the operating mode [18].

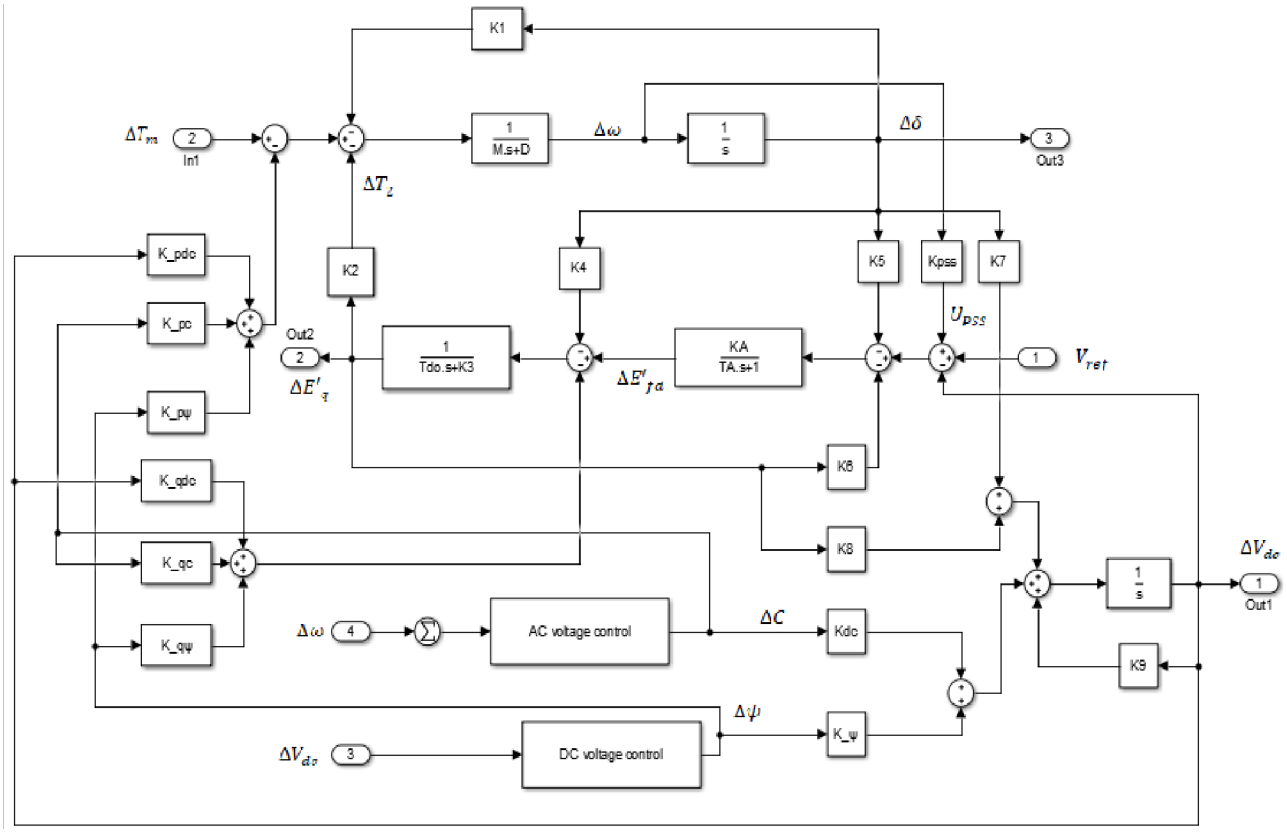

Figure 3. Linearized system with PSS and STATCOM.

5.1. Flou Controller Parameters

5.1.1. Fuzzification of Inputs

This initial step allows us to convert the numerical values of the input signals into fuzzy values, which means that these parameters will no longer be defined numerically, but in a *linguistic* manner. It involves defining a maximum allowed variation range for the input variables, which in our case correspond to the production limits and the rotational speed limits of a generator.

5.1.2. Membership Functions

Let's define the membership functions for the fuzzification of the measured values of active power and rotation speed [18] [19] [20]. We use five triangular membership functions for each variable, namely rotation speed and rotor angle. These functions are as follows: large negative (ng), small negative (np), zero (ze), small positive (pp), large positive (pg). **Figure 4** illustrates these different membership functions for the input variables and the output signal.

The inference stage corresponds to the decision-making of our adaptation block based on the two input variables. Fuzzy logic simplifies this decision-making by qualifying the inputs with quantitative terms [8] [20]. **Table 1**, below summarizes the twenty-five possible output states based on the inputs.

5.1.3. Defuzzification

The center of gravity method is used in the development of the adaptation block.

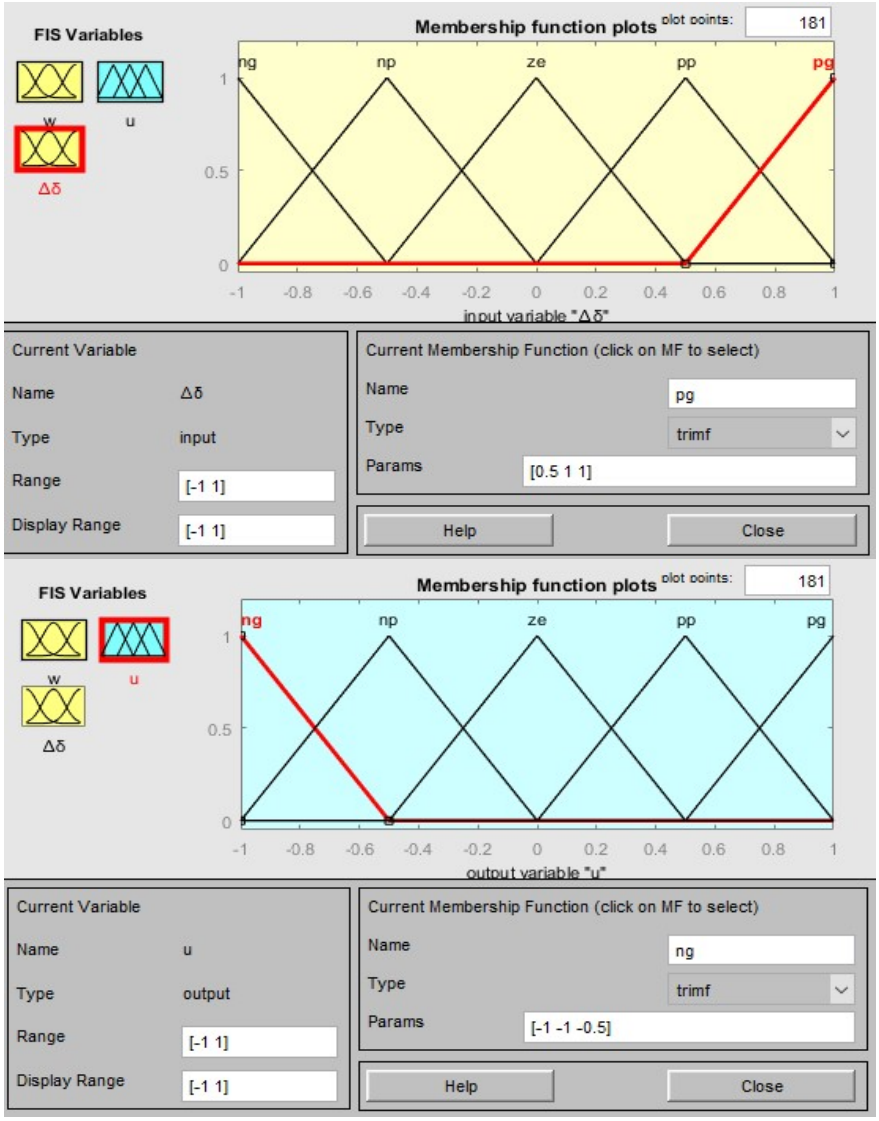

Figure 4. Membership functions of (ω, $\Delta\delta$) and u.

Table 1. Inference rules.

$\Delta\omega$	$\Delta\delta$				
	ng	np	ze	pp	pg
ng	ng	ng	ng	np	ze
np	ng	np	np	ze	pp
ze	ng	np	ze	pp	Pg
pp	np	ze	pp	pp	Pg
pg	ze	pp	pg	pg	pg

To evaluate the performance and robustness of the setting, it is necessary to analyze the new eigenvalues of the system and examine the damping obtained with the optimized PSS and STATCOM. Figure 5 below illustrates the proposed conceptual control scheme.

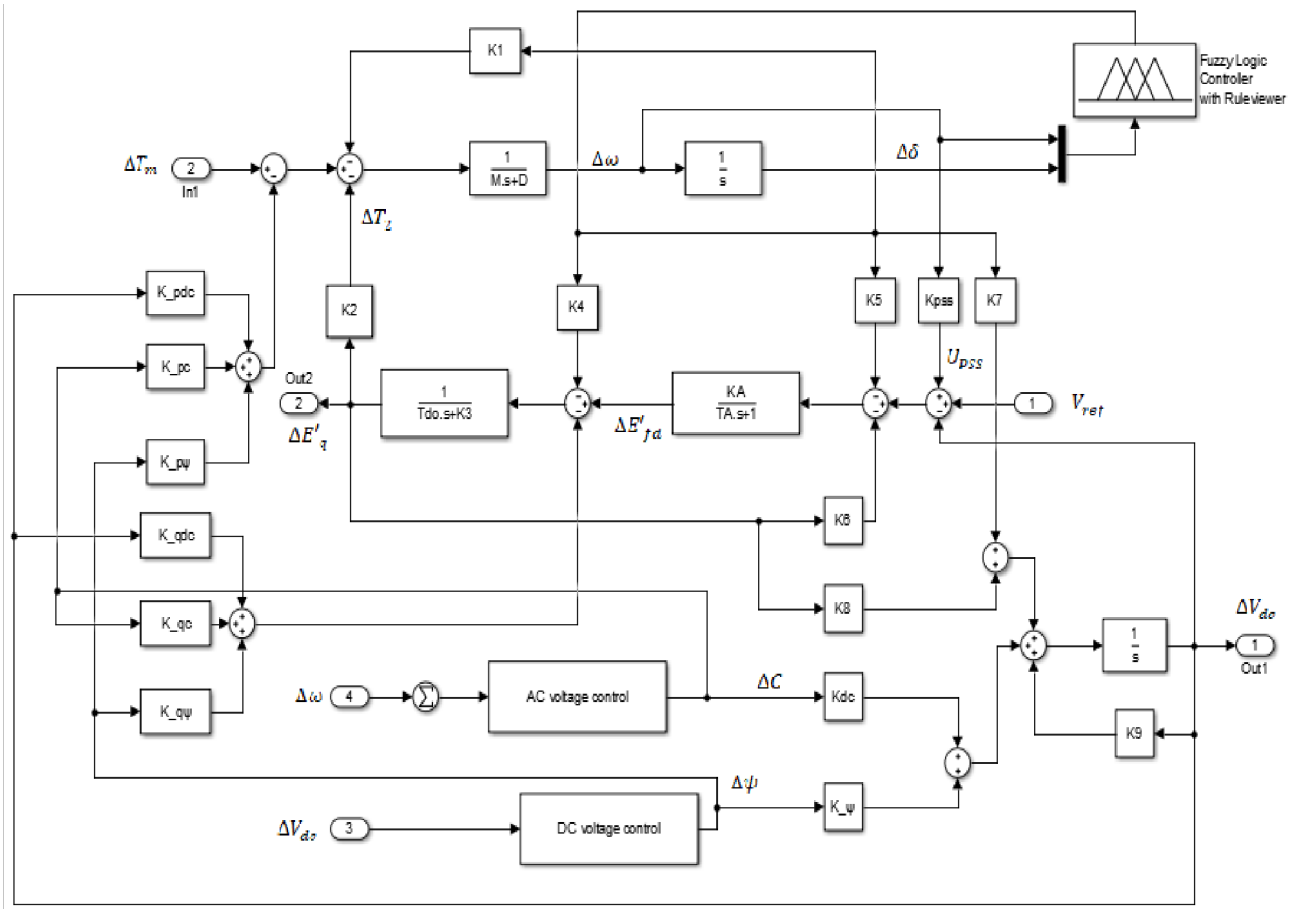

Figure 5. Conceptual diagram of LF control.

6. Description of the Electrical Network of the Republic of Congo

The single-line representation of the power transmission network of the Republic of Congo is a schematic representation that allows visualizing all the components of this network (**Figure 6**). This representation highlights the different power generation plants, loads, transmission lines, and nodes that make up this network. Specifically, the electric transmission network of the Republic of Congo is composed of five power generation plants. These plants are infrastructure that generates electricity to supply the country. They are strategically distributed across the territory to ensure a balanced and suitable production for the energy needs. The network also consists of 22 loads, which correspond to the places where electricity is consumed. These loads are mainly localities. The 24 transmission lines are the infrastructure that carries the electricity produced by the plants to the loads. These lines are often of long distances, which requires careful planning to ensure the reliability of the power distribution. Finally, the 35 nodes are the places where the transmission lines converge. These are strategic points of the network where electricity can be redistributed in different directions. These nodes allow for the creation of a meshed power network, which ensures better supply security in case of failure or malfunction. The geographical and

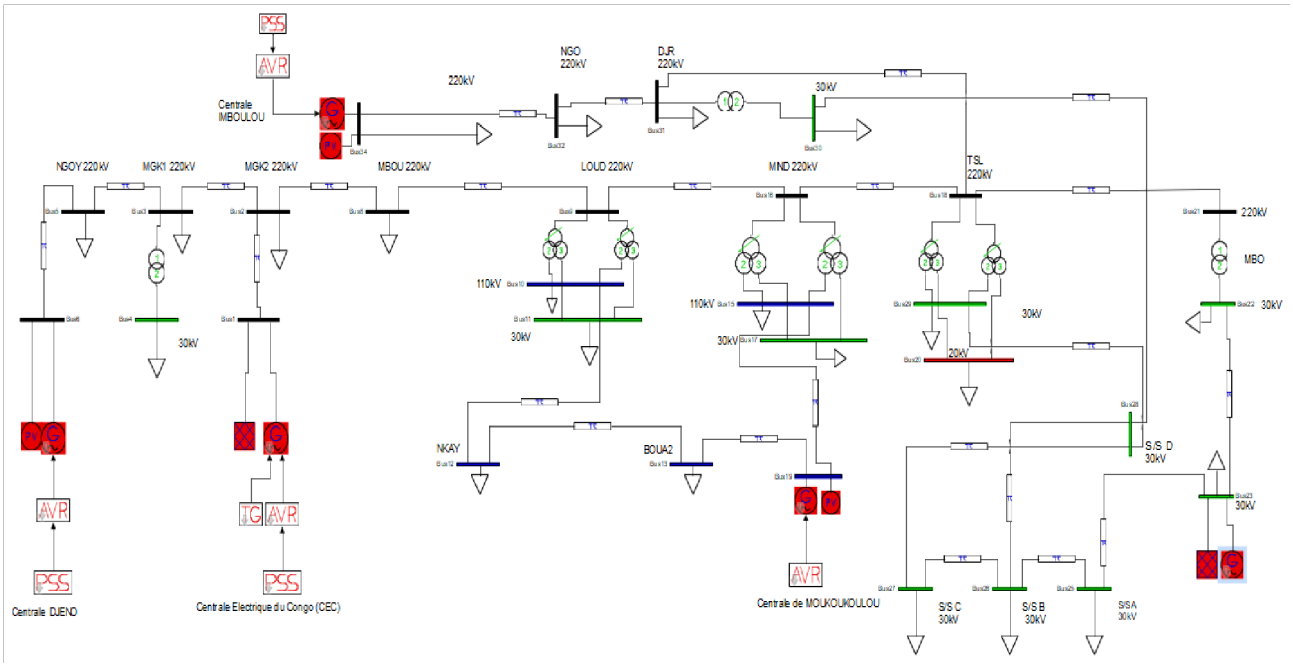

Figure 6. Power transmission network of the Republic of Congo.

schematic representation of the power transmission network of the Republic of Congo allows for a clear and precise visualization of all these elements. It provides an overview of the network and facilitates its management and maintenance.

7. Results

In this section, we begin by presenting the results of the analysis of the linear model of the electrical network in the Republic of Congo with power stabilizing devices (PSS) and static reactive power compensations (STATCOM), without the use of the fuzzy controller. We use the first method of Lyapunov to analyze the eigenvalues of the state matrix of the Congolese electrical network. Secondly, we perform coordination using a fuzzy logic controller that takes into account the rotational speed and angle of the electrical network as input variables.

7.1. Electric Grid with PSS-STATCOM

In this section, we will start by presenting the thermal profile of the voltage across all the nodes of the electric network of the Republic of Congo (RC). Then, we will present the results of the eigenvalue analysis of the state matrix of the RC's electrical network, where we will determine the different oscillation modes.

7.1.1. Power Flow

Figure 7 shows the voltage profile of all the nodes of the RC's electrical network with PSSSTATCOM without coordination.

According to Figure 7, it can be observed that the voltages in Brazzaville remain within acceptable limits. The STATCOMs have an impact not only on the connection node, but their effect is also felt on the neighboring nodes. However,

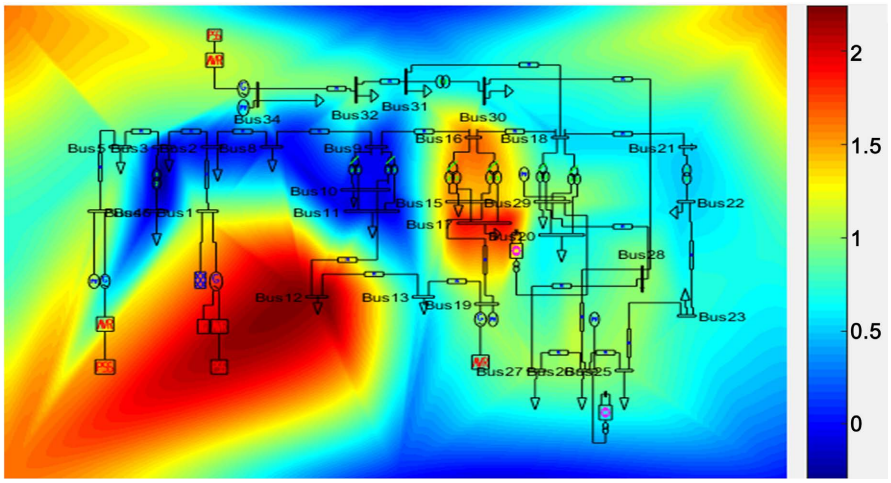

Figure 7. Electrical grid voltage of the RC with PSS-STATCOM without CF.

in the Pointe Noire area, from Loudima to Mongokamba 1, there is a decrease in voltage compared to the case where the RC's electrical network operates without STATCOM. In the Bouenza department, there is a voltage spike to note, particularly in the locality of Nkayi, with an exceeding value of 2pu.

7.1.2. Evolution over Time of Different Quantities

Voltages at the nodes of the generators

Figure 8 shows the voltages at the nodes of the generators.

In Figure 8, we observe that the voltages at the nodes of the generators stabilize after a few oscillations at $t = 14$ s. The evolution of the generator powers is shown in Figure 9.

Active powers at generator nodes

The electrical power produced by a power plant depends on the output voltage of thegenerator and the angle of the rotor. Figure 9 below illustrates the evolution over time of the transport power at the nodes of each generator.

It can be observed that in Figure 9, the evolution of power at the generator nodes remains almost constant. Figure 10 illustrates the rotation speeds of each generator in the Republic of Congo's electrical network.

Figure 10 represents the rotation speeds of the generators, which gradually decrease until reaching a constant value of 0.95.

7.1.3. Eigenvalues without CF

Figure 11 displays the eigenvalues of the electrical network with PSS-STATCOM.

Figure 11 reveals that all the eigenvalues are located in the negative real part of the complex plane. However, it is important to note the presence of an unstable mode, indicated in red on this figure.

7.2. Results of the Power Grid in the RC with Fuzzy Control

In this section, we have implemented a coordination of PSS-STATCOM control devices using fuzzy logic. Table 2 presents the various scenarios that we have

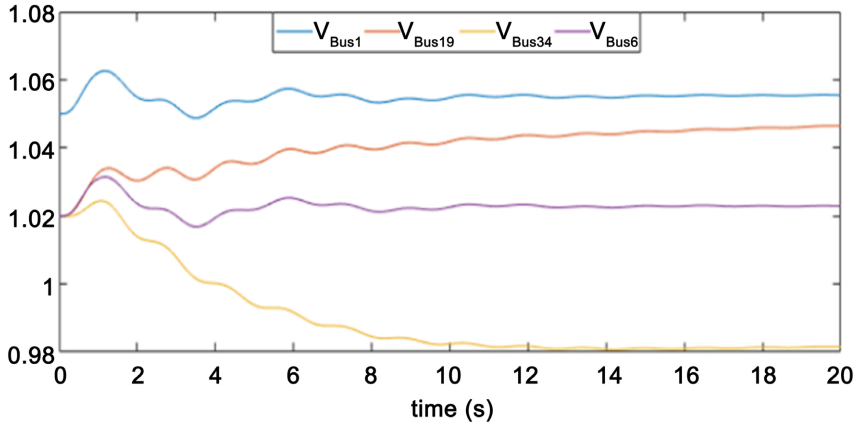

Figure 8. Tension at the nodes of generators without flow control. V_{b1}: Congo Power Plant.; V_{b34}: Imboulou; V_{b8}: Djeno; V_{b19}: Moukoukoulou.

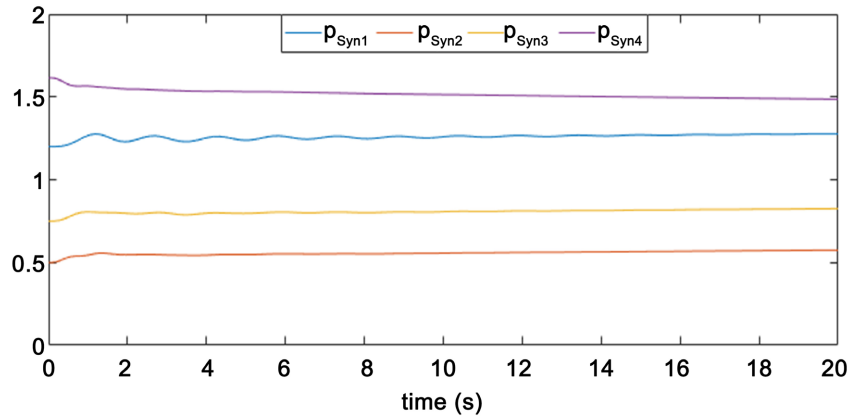

Figure 9. Active powers at generator nodes without CF.

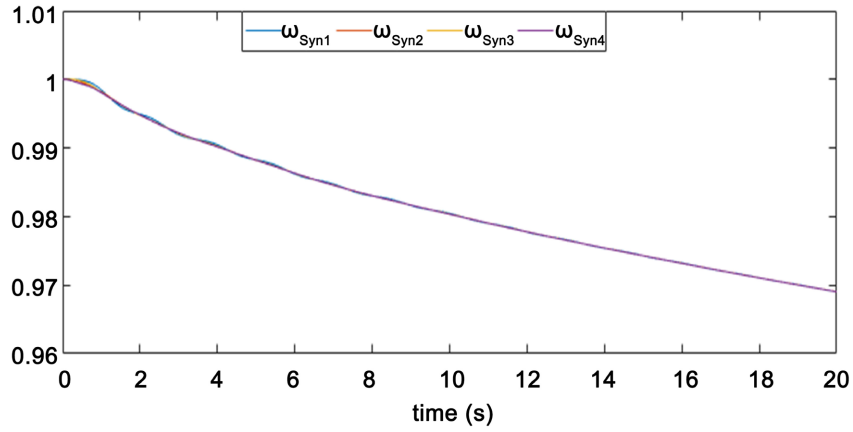

Figure 10. Speed rotation of generators with PSS-STATCOM without CF.

Table 2. List of scenarios.

Scenario	Scenario configuration
1	10% decrease in the active power of generator 1 (CEC)
2	Increase of 20% in the active power of the load at node 13

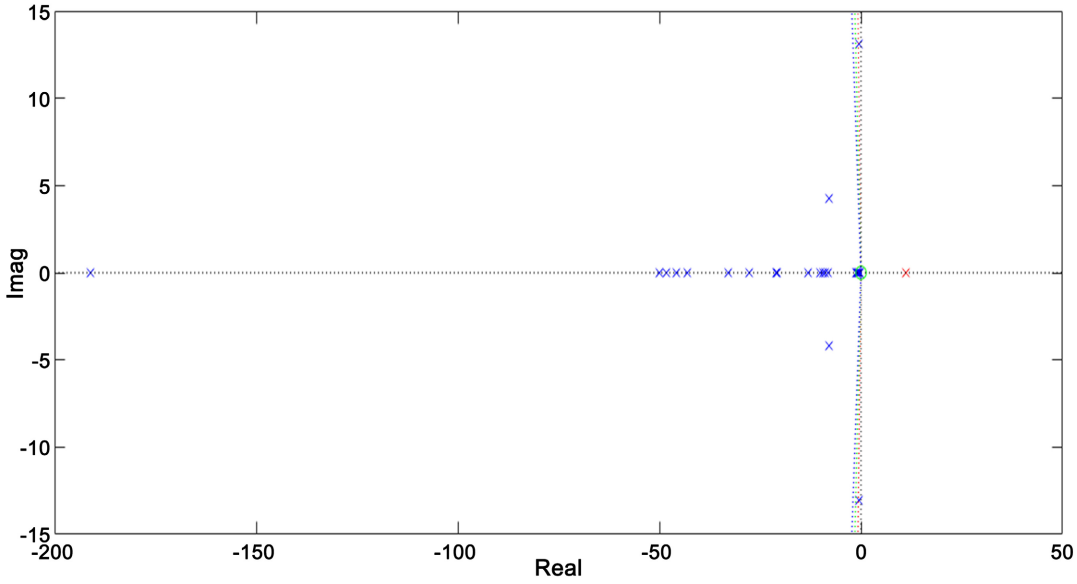

Figure 11. Eigenvalues of the power system with PSS-STATCOM in the complex plane.

developed to assess the behavior of the electrical network during dynamic disturbances.

7.2.1. Temporal Simulation Analysis

The variation in generator speed in response to a 15% reduction in generator power at the Congo power plant (node 1) and a 20% increase in load at Bouenza (node 13) is presented in **Figure 12**.

In **Figure 12**, we observe the evolution of the rotation speed of the generators of the different power plants. It is clear that the 10% reduction in active power of the generator at the Congo Electric Power plant (CEC) and the 20% increase in active power at node 13 lead to a gradual decrease in the rotation speed of all the generators in the network. **Figure 13** below presents the temporal evolution of the power of the generators of the different power plants.

Figure 13 shows the electrical powers of the generators. This evolution of powers in the case of the different scenarios mentioned above allows us to observe the efficiency of coordination through fuzzy logic. We can see that the power evolution of the CEC and Imboulou power plants is disrupted in the first ten seconds ($tp = 10\ s$), but then returns to normal operation. On the other hand, the Moukoukoulou power plant (in red) and the Djéno power plant (in green) show more pronounced power fluctuations in terms of amplitudes, for a duration of about twenty seconds ($tp = 10\ s$). This can be explained by the 20% increase in load at node 13, located near the Moukoukoulou power plant. **Figure 14** shows the evolution of node voltages for the different generators.

Figure 14 shows the evolution of the voltages at the generator nodes of the various power plants. We can see that the disturbed voltages evolve over time. However, the response time does not exceed ten seconds (10 s) to bring the voltages progressively back to the reference voltage 1 pu. As can be seen from the

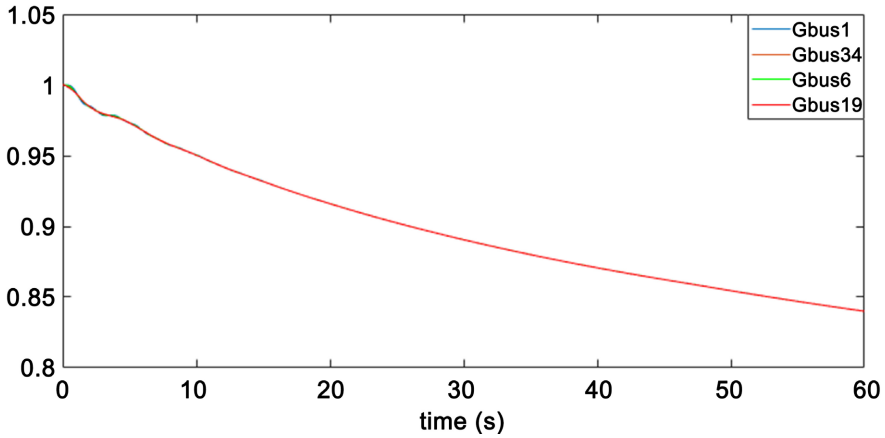

Figure 12. Variation of speed of the five generators with CF.

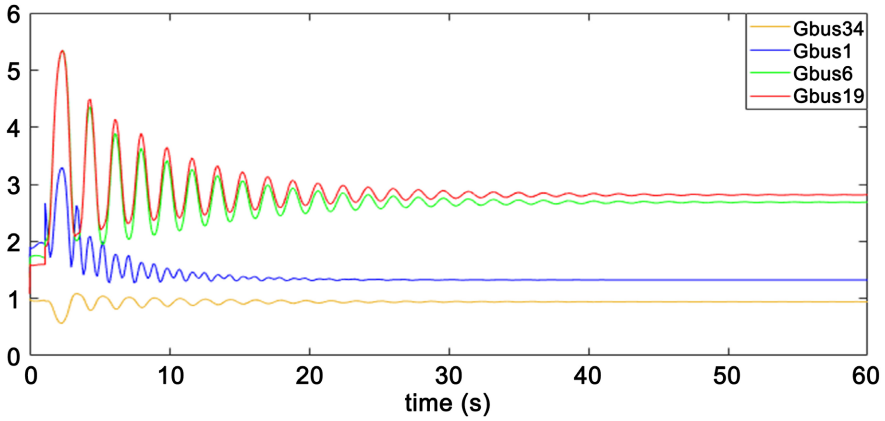

Figure 13. Electrical power of generators with CF.

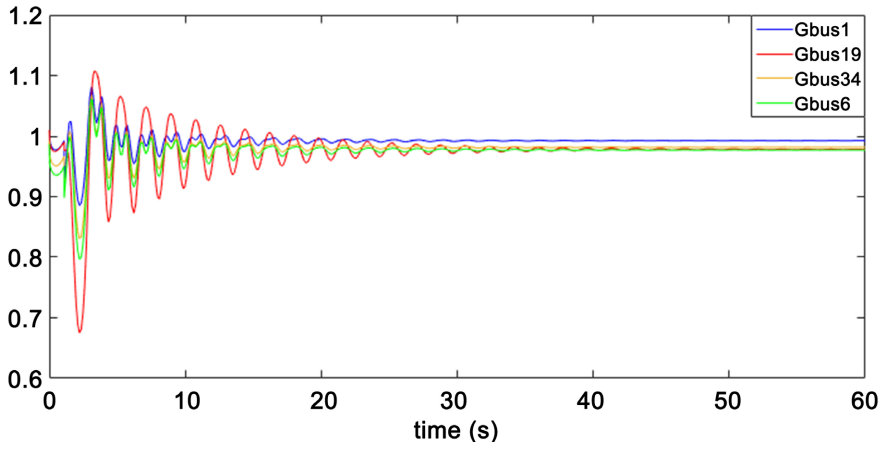

Figure 14. Node voltages of generators with CF.

previous figures, the terminal voltage of the Moukoukoulou power plant shows the greatest fluctuation, with a voltage drop recorded at (0.7 pu). **Figure 15** below illustrates the evolution of currents in the two statcom shunt compensators, inserted at nodes 25 and 28 respectively.

We observe in Figure 15 that the current of STATCOM 1 undergoes a sudden disturbance in the first ten (10) seconds. However, this disturbance in the current of STATCOM 1 disappears and settles at the value of 0.2 pu. We also observe in this figure that the current of STATCOM 2 only shows a slight variation, which disappears within five (05) seconds and subsequently settles at the value of 0.1 pu. Figure 16 below illustrates the variations in the real value of the controller's output signal as a function of the inputs when these latter traverse the universe of discourse.

7.2.2. Eigenvalues with CF

In this section, Figure 17 presents the distribution of the different eigenvalues in the complex plane with coordinated control using fuzzy logic.

Figure 17 illustrates the different eigenvalues in the complex plane. It can be easily observed that there are no unstable modes. This is explained by the fact that all modes have a negative real part.

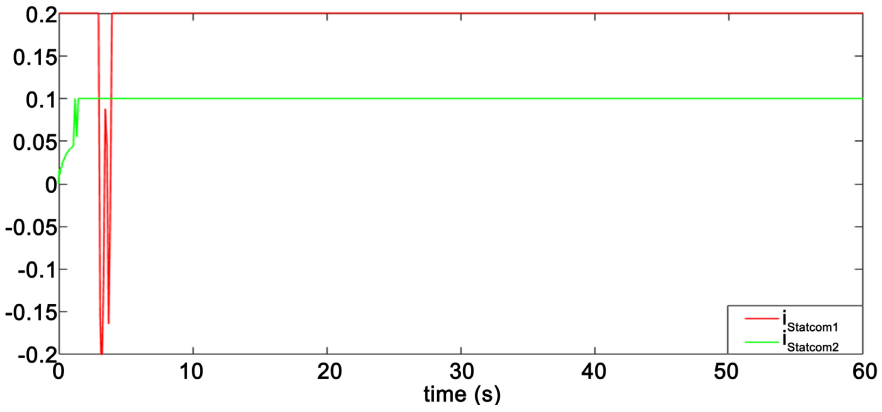

Figure 15. Variations of STATCOM currents.

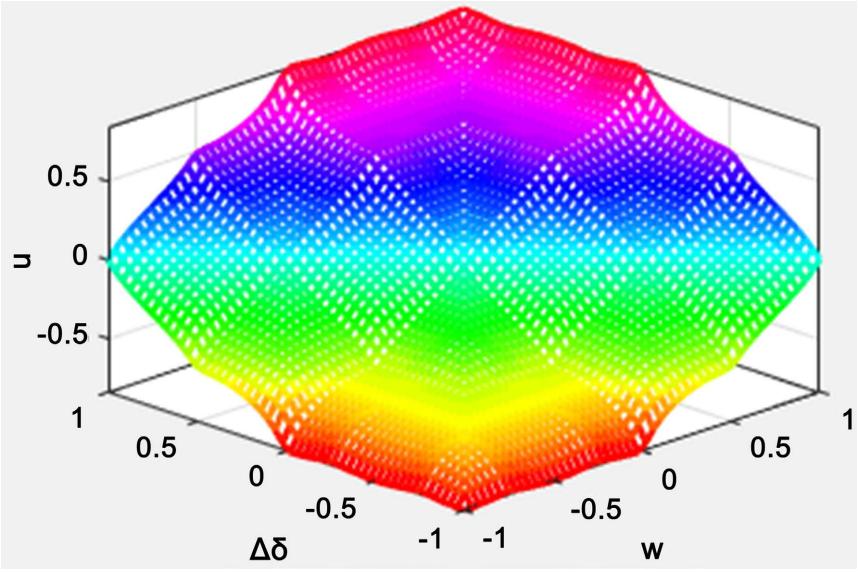

Figure 16. Characteristic surface of the controller.

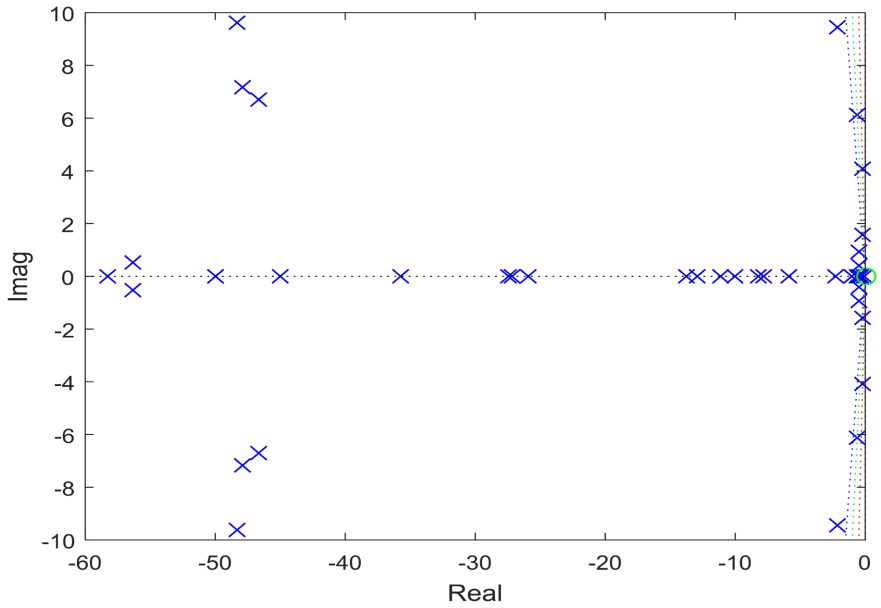

Figure 17. Eigenvalues with PSS-STATCOM in the complex plane with CF.

8. Conclusion

In conclusion, our study allowed us to analyze and improve the stability of the electrical network in the Republic of Congo by using PSS-STATCOM devices with and without fuzzy logic control. We found that the absence of coordinated control led to undesirable interactions and unstable oscillation phenomena. However, by applying fuzzy logic to coordinate the regulation devices, we were able to optimize the interactions and improve the efficiency of network stabilization. These results highlight the importance of coordinated and intelligent control in the field of management and operation of transmission electrical networks, and demonstrate the advantages of using fuzzy logic in the presence of multiple PSS and STATCOM devices. Our work paves the way for future studies aimed at further improving the stability of the electrical network in the Republic of Congo and assessing the large-scale impact of these coordinated regulation devices on the distribution network.

Conflicts of Interest

The authors declare no conflicts of interest regarding the publication of this paper.

References

[1] Wang, H.F. and Swift, F.J. (1997) A Unified Model for the Analysis of FACTS Devices in Damping Power System Oscillations Part I: Single-Machine Infinite-Bus Power Systems. *IEEE Transactions on Power Delivery*, **12**, 941-946. https://doi.org/10.1109/61.584417

[2] Padiyar, K.R. (2006) Investigation on Strong Resonance in Multimachine Power Systems with STATCOM Supplementary Modulation Controller. *IEEE Transactions on Power Systems*, **21**, 754-762. https://doi.org/10.1109/TPWRS.2006.873405

[3] Kundur, P. (1994) Power System Stability and Control. McGraw-Hill, New York.

[4] Rodrigo, A.R. (2009) Stability Analysis of Power Systems Considering AVR and PSS Output Limiters. *International Journal of Electrical Power & Energy Systems*, **31**, 153-159. https://doi.org/10.1016/j.ijepes.2008.10.017

[5] Passelergue, J.C. (1998) Interactions des dispositifs FACTS dans les grands réseaux élec-triques. Thèse de doctorat, Institut National Polytechnique de Grenoble.

[6] Ammari, S. (2000) Interaction des dispositifs FACTS avec les charges dynamiques dans les réseaux de transport et d'interconnexion. Thèse de doctorat en Génie Electrique, INPG.

[7] Soto, D. and Pena, R. (2004) Non Linear Control Strategies for Cascaded Multilevel Statcom. *IEEE Transactions on Power Delivery*, **19**, 1919-1927. https://doi.org/10.1109/TPWRD.2004.835394

[8] Karuppiah, N., Malathi, V. and Selvalakshmi, G. (2014) Transient Stability Enhancement Using Fuzzy Controlled SVC and STATCOM. *International Journal of Innovative Research in Science*, *Engineering and Technology*, **3**, 2319-8753.

[9] Mak, L.O., Ni, Y.X. and Shen, C.M. (2000) Statcom with Fuzzy Controllers for Interconnected Power Systems. *Electric Power Systems Research*, **55**, 87-95. https://doi.org/10.1016/S0378-7796(99)00100-5

[10] Bougouffa, L. (2016) Effets des Systèmes de Compensation FACTS sur la Protection à Maximum de Courant dans les Réseaux Électriques. Thèse de doctorat, Université de Batna 2 Faculté de Technologie.

[11] Sasidharan, S., Tibin, J., Sebin, J., Chittesh, V.C., Vishnu, J. and Vipin, D. (2019) Power System Loading Margin Enhancement by Optimal STATCOM Integration—A Case Study. *Computers & Electrical Engineering*, **81**, Article ID: 106521.

[12] Bhargava, B. and Dishaw, G. (1998) Application of an Energy Source Power System Stabilizer on the 10 MW Battery Energy Storage System at Chino Substation. *IEEE Transaction on Power System*, **13**, 145-151. https://doi.org/10.1109/59.651626

[13] Wu, C.-J. and Hsu, Y.Y. (1998) Design of Self-Tuning PID Power System Stabilizer for Multimachine Power Systems. *IEEE Transactions on Power Systems*, **3**, 1059-1064. https://doi.org/10.1109/59.14562

[14] Tharani, A.S. and Jyothsna, T.R. (2010) Design of PSS for Small Signal Stability Improvement. 16*th National Power Systems Conference*, Hyderabad, 15-17 December 2010, 641-646.

[15] Lin, K.M. and Swe, W.P.L. (2013) Coordinated Design of PSS and STATCOM for Power System Stability Improvement Using Bacteria Foraging Algorithm. *International Journal of Electrical*, *Computer*, *Electronics and Communication Engineering*, **7**, 205-2012.

[16] Mondal, D., Chakrabarti, A. and Sengupta, A. (2020) Power System Small Signal Stability Analysis and Control. Library of Congress Cataloging-in-Publication Data Application Submitted, First Edition, Elsevier Inc., San Diego.

[17] Bati, A.F. (2010) Optimal Interaction between PSS and FACTS Devices in Damping Power Systems Oscillations: Part II. *IEEE International Energy Conference*, Manama, 18-22 December 2010, 452-457. https://doi.org/10.1109/ENERGYCON.2010.5771723

[18] Abu-Tabak, N. (2008) Stabilité dynamique des systèmes électriques multima-chines: modélisation, commande, observation et simulation. Thèse de doctorat. https://theses.hal.science/tel-00343722v2

[19] Passino, K.M., Yurkovich, S. and Reinfrank, M. (1998) Fuzzy Control. Vol. 42, Ad-

dison-Wesley, California, 15-21. https://doi.org/10.1109/13.746327

[20] Narne, R. and Panda, P.C. (2012) Optimal Coordinate Control of PSS with Series and Shunt FACTS Stabilizers for Damping Power Oscillations. *IEEE International Conference on Power Electronics, Drives and Energy Systems*, Bengaluru, 16-19 December 2012, 16-19. https://doi.org/10.1109/PEDES.2012.6484430

Appendices

Table A1. Parameters of the generators in the RC network.

Générateurs	X_d	X'_d	T'_{d0}	X_q	H
CEC	2.42	0.23	10.8	2.25	5.09
Imboulou	1.00	0.29	4.54	0.64	6
Djéno	2.02	0.19	6.9	1.9	5
Moukoukoulou	1.14	0.28	5	0.8	6

Table A2. Parameters of the regulation systems [16].

Power System Stabilizer	$K_{PSS}=4$; $T_1=T_2=T_3=T_4=0.5\,\text{s}$
Excitation system	$K_A=200$; $T_A=0.02$
STATCOM	$K_P=0.8$; $K_1=50$; $T_1=0.2\,\text{s}$; $T_2=0.1\,\text{s}$